

Halo Effect in the Coulomb-Modified Eikonal Model Analysis for $^{11}\text{Li}+p$ Elastic Scattering

Yong Joo Kim

Department of Physics, Cheju National University, Jeju 690-756

The elastic scattering of $^{11}\text{Li}+p$ at $E_{\text{lab}}/A = 62$ MeV/nucleon has been analyzed within the framework of Coulomb-modified eikonal model based on hyperbolic trajectory. It is assumed that ^{11}Li has a halo structure of a ^9Li core plus two weakly bound neutrons and is treated that the total nuclear optical potential as a sum of core and halo neutron contributions. The theoretical calculation for the elastic scattering cross section of $^{11}\text{Li}+p$ at $E_{\text{lab}}/A = 62$ MeV/nucleon provide a reasonable agreements with the experimental data. We have found that break-up effect of halo neutrons is important to understand the elastic cross sections of $^{11}\text{Li} + p$ system at $E_{\text{lab}}/A = 62$ MeV/nucleon.

I. INTROCUCTION

The invention and development of the radioactive ion beam has made possible to search for experimental evidences of neutron halos. The studies of elastic scattering of neutron rich nuclei have attracted much interest of nuclear physicists in the past two decades. The halo structure of the nuclei with large neutron-to-proton ratio has been studied [1-10] extensively. The structure and reactions of ^{11}Li nucleus has attracted much experimental and theoretical interest as a typical case. It has been found that light neutron-rich nuclei, such as ^{11}Li , have a neutron halo, which is a spatially prolonged distribution of valence neutrons, extending far beyond a well-defined core nucleus.

Proton elastic scattering cross sections of ^9Li and ^{11}Li at $E_{\text{lab}}/A=60$ and 62 MeV/nucleon, respectively, have been measured and analyzed using the phenomenological optical model [3]. The elastic scattering of weakly bound projectiles such as deuteron and ^{11}Li nucleus are examined [4] including the break-up process to the continuum excited states. Hirenzaki *et al.* [5] have studied the proton elastic scattering of ^9Li and ^{11}Li using the Born approximation and the optical potential approach. For the proton- $^{9,11}\text{Li}$ elastic scattering, the importance of the central and spin-orbit terms of the optical potential, and of the core and halo nucleon contributions was clarified based on the single scattering approximation to the Kerman-McManus-Thaler multiple scattering expansion [8]. The proton elastic scattering of ^{11}Li

has been analyzed within the framework of an extended Glauber model to take into account the neutron halo effect [11].

Over the last decades, eikonal approximation has been established as a useful tool for the study of heavy-ion elastic scattering. The phase shifts in the eikonal approximation are derived from the integral equation by further approximation the WKB results [12]. A number of studies [13-16] have been made to describe elastic scattering processes between heavy ions within the framework of the eikonal approximation methods. Cha and Kim [17] have presented the first- and second-order corrections to the zero-order eikonal phase shifts for heavy-ion elastic scatterings based on Coulomb trajectories of colliding nuclei and it has been applied satisfactorily to the $^{16}\text{O} + ^{40}\text{Ca}$ and $^{16}\text{O} + ^{90}\text{Zr}$ systems at $E_{\text{lab}}=1503$ MeV.

The Glauber model approach based on hyperbolic trajectory for the description of the heavy-ion reaction cross section has been presented to extend to lower energies [18]. In this Glauber model, trajectory modifications due to the nuclear potential apart from the Coulomb potential has been suggested by Gupta and Shukla [19]. The Coulomb-modified eikonal model formalism based on hyperbolic trajectory for the description of heavy-ion elastic scattering was described and it has been applied satisfactorily to elastic scatterings of $^{12}\text{C} + ^{12}\text{C}$ system at $E_{\text{lab}}=240, 360$ and 1016 MeV [20].

In our previous paper [21], we have analyzed the elastic scatterings of $^9\text{Li}+p$ and $^{11}\text{Li}+p$ systems at $E_{\text{lab}}/A=60$ and 62 MeV/nucleon, respectively, by using the

Coulomb-modified eikonal model based on Coulomb trajectory. In this paper, we present the Coulomb-modified eikonal model based on hyperbolic trajectory to take into account the halo effect and apply it to the $^{11}\text{Li}+p$ systems at $E_{\text{lab}}/A = 62$ MeV/nucleon. Assuming that the ^{11}Li nucleus has a halo structure of two weakly bound neutrons around the ^9Li core nucleus, we take the optical potential of ^9Li as the core potential for ^{11}Li and add a halo potential arising from the two weakly bound neutrons. In section II, we present the theory related with the Coulomb-modified eikonal model based on hyperbolic trajectory. Section III contains results and discussions. Finally, concluding remarks are presented in section 4.

II. THEORY

If there is a single turning point in the radial Schrödinger equation, a first-order WKB expression for the nuclear elastic phase shifts δ_L , taking into account the deflection effect due to Coulomb field, can be written as [14, 15]

$$\delta_L = \int_{r_t}^{\infty} k_L(r) dr - \int_{r_c}^{\infty} k_c(r) dr, \quad (1)$$

where r_t and r_c are the turning points corresponding to the local wave numbers $k_L(r)$ and $k_c(r)$ given by

$$k_L(r) = k \left[1 - \left(\frac{2\eta}{kr} + \frac{(L + \frac{1}{2})^2}{k^2 r^2} + \frac{U_N(r)}{E} \right) \right]^{1/2}, \quad (2)$$

$$k_c(r) = k \left[1 - \left(\frac{2\eta}{kr} + \frac{(L + \frac{1}{2})^2}{k^2 r^2} \right) \right]^{1/2}, \quad (3)$$

where $k = \sqrt{2\mu E}/\hbar$, η is the Sommerfeld parameter, and $U_N(r)$ the nuclear potential. If

we consider the nuclear potential as a perturbation, the nuclear phase shift can be written as

$$\delta(r_c) = -\frac{\mu}{\hbar^2 k} \int_{r_c}^{\infty} \frac{r U_N(r)}{\sqrt{r^2 - r_c^2}} dr, \quad (4)$$

where r_c is the distance of closest approach given by

$$r_c = \frac{1}{k} \left\{ \eta + \left[\eta^2 + (L + \frac{1}{2})^2 \right]^{1/2} \right\}, \quad (5)$$

and r is given in the cylindrical coordinate system as

$$r^2 = y^2 + z^2. \quad (6)$$

In the heavy-ion scattering, the orbit describing a projectile may be considered as one branch of a hyperbola. The hyperbolic trajectory with respect to the center of the potential in case of the Coulomb potential is given by [19]

$$\frac{k^2(y-s)^2}{\eta^2} - \frac{k^2 z^2}{L^2} = 1, \quad (7)$$

where

$$s = (\eta^2 + L^2)^{1/2}/k. \quad (8)$$

By arranging Eq. (7), the following expression is obtained

$$y^2 = r_c^2 + \frac{2s\eta}{k} \left(\sqrt{1 + \frac{k^2}{L^2} z^2} - 1 \right) + \frac{\eta^2}{L^2} z^2. \quad (9)$$

From Eqs. (4), (6) and (9), the nuclear phase shift $\delta_L(r_c)$ can further be expressed as

$$\delta_L(r_c) = -\frac{\mu}{\hbar^2 k} \int_0^{\infty} \frac{\left[\frac{s\eta k}{L^2} \frac{1}{\sqrt{1 + k^2 z^2/L^2}} + (\frac{\eta^2}{L^2} + 1) \right] U_N(r)}{\left[\frac{2s\eta}{k} (\sqrt{1 + k^2 z^2/L^2} - 1) + (\eta^2/L^2 + 1) z^2 \right]^{1/2}} dz. \quad (10)$$

In the $^{11}\text{Li} + p$ elastic scattering, the halo nucleus (^{11}Li) is treated as a (core nucleus) + (halo neutrons) system interacting with the proton through (core nucleus) - and (halo neutrons)- proton interactions. Then, the optical potential can be given as a sum of core nucleus and two halo neutrons contributions,

$$U_N(r) = U_c(r) + U_h(r), \quad (11)$$

where $U_c(r)$ and $U_h(r)$ are the optical potential for (core nucleus + p) and (halo neutrons + p), respectively. So, the nuclear phase shift $\delta(r_c)$ including the effect of the halo neutrons break-up can further be written as

$$\begin{aligned} \delta(r_c) &= \delta_c(r_c) + \delta_h(r_c) \\ &= -\frac{\mu}{\hbar^2 k} \int_0^\infty \frac{\left[\frac{s\eta k}{L^2} \frac{1}{\sqrt{1+k^2 z^2/L^2}} + \left(\frac{\eta^2}{L^2} + 1\right) \right] U_c(r)}{\left[\frac{2s\eta}{k} (\sqrt{1+k^2 z^2/L^2} - 1) + (\eta^2/L^2 + 1) z^2 \right]^{1/2}} dz \\ &\quad - \frac{\mu}{\hbar^2 k} \int_0^\infty \frac{\left[\frac{s\eta k}{L^2} \frac{1}{\sqrt{1+k^2 z^2/L^2}} + \left(\frac{\eta^2}{L^2} + 1\right) \right] U_h(r)}{\left[\frac{2s\eta}{k} (\sqrt{1+k^2 z^2/L^2} - 1) + (\eta^2/L^2 + 1) z^2 \right]^{1/2}} dz. \end{aligned} \quad (12)$$

By taking $U_c(r)$ and $U_h(r)$ as the optical Woods-Saxon forms given by

$$U_c(r) = -\frac{V_0}{1 + e^{(r-R_v)/a_v}} - i \frac{W_0}{1 + e^{(r-R_w)/a_w}}, \quad (13)$$

and

$$U_h(r) = -\frac{V_0^h}{1 + e^{(r-R_v^h)/a_v^h}} - i \frac{W_0^h}{1 + e^{(r-R_w^h)/a_w^h}}, \quad (14)$$

we can use the phase shift in the general expression for the elastic scattering amplitude. Ignoring spin-orbit effects, the elastic scattering cross sections are then obtained from the scattering amplitude

$$\begin{aligned} f(\theta) &= f_R(\theta) + \frac{1}{ik} \sum_{l=0}^{\infty} \left(L + \frac{1}{2} \right) e^{2i\sigma_L} (S_L^N - 1) \\ &\quad \times P_L(\cos \theta), \end{aligned} \quad (15)$$

where $f_R(\theta)$ is the usual Rutherford scattering amplitude and σ_L the Coulomb phase shift. The nuclear S -matrix elements S_L^N in this equation can be expressed by the nuclear

phase shift δ_L as

$$S_L^N = e^{2i\delta_L}. \quad (16)$$

III. RESULTS AND DISCUSSIONS

As in the proceeding section, we have calculated the elastic differential cross section for $^{11}\text{Li} + p$ systems at $E_{\text{lab}}/A = 62$ MeV/nucleon by using the Coulomb-modified eikonal model based on hyperbolic trajectory. Table I show the least square fitted parameters of Woods-Saxon potential for $^9\text{Li} + p$ and $^{11}\text{Li} + p$ systems at $E_{\text{lab}}/A = 60$ and 62 MeV/nucleon in the Coulomb-modified eikonal model based on hyperbolic trajectory. In order to take into account the halo effect of ^{11}Li nucleus, we assume that ^{11}Li has a halo structure of two weakly bound neutrons around ^9Li core. Then, the total optical potential of $^{11}\text{Li} + p$ system can be treated as a sum of the core potential and two neutrons halo one. Since the core potential of $^{11}\text{Li} + p$

system is considered approximately the same as the one of ${}^9\text{Li} + p$ system, we have chosen the core potential obtained from fitting the ${}^9\text{Li} + p$ elastic scattering data at $E_{\text{lab}}/A=60$ MeV/nucleon given in table I. After fixing the core potential, the halo potential parameters are adjusted so as to minimize the χ^2/N

given by

$$\chi^2/N = \frac{1}{N} \sum_{i=1}^N \left[\frac{\sigma_{exp}^i - \sigma_{cal}^i}{\Delta\sigma_{exp}^i} \right]^2. \quad (17)$$

TABLE I: Parameters of the fitted Woods-Saxon potential in the Coulomb-modified eikonal model based on hyperbolic trajectory for ${}^9\text{Li}+p$ and ${}^{11}\text{Li}+p$ systems at $E_{\text{lab}}/A=60$ and 62 MeV/nucleon, respectively.

System	V_o (MeV)	R_v (fm)	a_v (fm)	W_o (MeV)	R_w (fm)	a_w (fm)	χ^2/N
${}^9\text{Li}+p$	35.0	2.27	0.62	25.2	2.16	0.52	0.87
${}^{11}\text{Li}+p$	33.8	2.42	0.68	21.8	2.31	0.80	1.84

TABLE II: The halo part of optical potential parameters in the Coulomb-modified eikonal model based on hyperbolic trajectory for ${}^{11}\text{Li}+p$ elastic scattering at $E_{\text{lab}}/A=62$ MeV/nucleon. The core part of optical potential is taken from ${}^9\text{Li}+p$ system at $E_{\text{lab}}/A=60$ MeV/nucleon given in table I.

V_o^h (MeV)	R_v^h (fm)	a_v^h (fm)	W_o^h (MeV)	R_w^h (fm)	a_w^h (fm)	χ^2/N
28.8	0.83	0.49	15.3	1.40	1.27	1.11

In Eq.(17), σ_{exp}^i (σ_{cal}^i) and $\Delta\sigma_{exp}^i$ are the experimental (calculated) cross sections and uncertainties, respectively, and N is the number of data used in the fitting. The fitted halo Woods-Saxon potential parameters are given in table II. The calculated results for elastic angular distributions of the ${}^9\text{Li}+p$ and ${}^{11}\text{Li}+p$ systems at $E_{\text{lab}}/A=60$ and 62 MeV/nucleon, respectively, are presented in Fig. 1 together with the observed data [3]. The dashed curves in Figs. 1(a) and 1(b) are the calculated cross sections obtained from the common eikonal model based on hyperbolic trajectory by using the optical potential

given in Table I, while the solid curve in Fig. 1(b) is the calculated result including the halo potential given in Table II. As shown in Fig. 1, the experimental data are reasonably reproduced in both cases. In particular, eikonal model based on hyperbolic trajectory including the halo effect can provide an overall good description of elastic cross section of ${}^{11}\text{Li}+p$ systems at $E_{\text{lab}}/A=62$ MeV/nucleon, compared with one without halo one. It can see in table I and II that value of χ^2/N for ${}^{11}\text{Li}+p$ system at $E_{\text{lab}}/A=62$ MeV/nucleon decrease in the calculated result including the halo, compared to the value without halo one.

More realistic insight into the phenomena of angular distributions for the ${}^9\text{Li}+p$ and ${}^{11}\text{Li}+p$ systems at $E_{\text{lab}}/A=60$ and 62 MeV/nucleon, respectively, can be provided

by the representation of the elastic scattering amplitude in terms of the near- and far-side components. The near- and far-side decompositions of the scattering amplitude in the

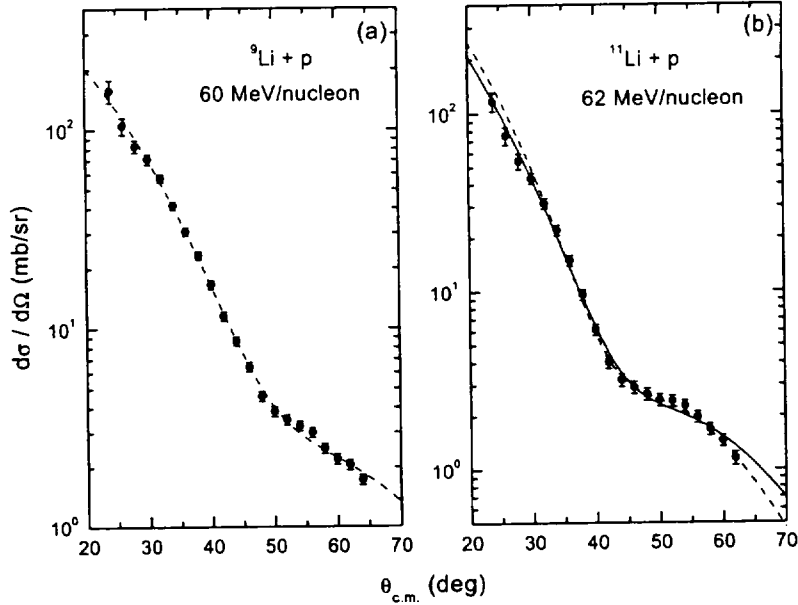


FIG. 1: Elastic scattering angular distributions for ${}^9\text{Li} + p$ and ${}^{11}\text{Li} + p$ systems at $E_{\text{lab}}/A=60$ and 62 MeV/nucleon, respectively. The solid circles represent the observed data taken from Ref. [3]. The dashed curves are the calculated results obtained from the common Coulomb-modified eikonal model based on hyperbolic trajectory, while the solid curve is the calculated one including the halo effect.

Coulomb-modified eikonal model based on hyperbolic trajectory were performed by the Fuller's formalism [22]. The contributions of the near- and far-side components to the elastic cross sections with the Coulomb-modified eikonal model based on hyperbolic trajectory for ${}^9\text{Li} + p$ and ${}^{11}\text{Li} + p$ systems, respectively, are shown in figures 2(a) and 2(b) along with the total differential cross section. The figure 2(a) are the results obtained from the common Coulomb-modified eikonal model, while figure 2(b) are the calculated ones using the eikonal model including the break-up effect. The total differential cross section is not just a sum of the near- and far-side components but contains very small interference between the two amplitudes as seen in figures. 2(a) and 2(b). In both cases, the near-side amplitudes corresponding to the positive-angle trajectories are very small compared with the far-side one over the whole angle. So, the elastic scattering patterns of these systems

are dominated by the refraction of the far-side trajectories. The angular distributions for ${}^9\text{Li} + p$ and ${}^{11}\text{Li} + p$ systems at $E_{\text{lab}}/A = 60$ and 62 MeV/nucleon, respectively, show very weak oscillations due to the smallness of the near components.

To investigate the neutron halo effect in ${}^{11}\text{Li} + p$ system at $E_{\text{lab}}/A = 62$ MeV/nucleon, we plotted the real and imaginary parts of the core and halo contributions to the optical potentials, along with the total ones in figure 3. As is expected, the halo potentials are small compared to core potential. The halo contribution to the real potential is negligibly. But we can in Fig. 3(b) see the larger value of the imaginary part of the core potential compared with the halo one in the interior region. Since most of the contribution to the differential cross section comes from the surface region of the colliding nuclei, the discrepancy between those imaginary parts in the interior region can be neglected. However, imaginary

halo potential give a significant contribution in the outer regions of the potential. This fact indicates that the elastic scattering of $^{11}\text{Li}+p$ system can be described as a sum of core potential and imaginary halo one. This results

are consistent with one of Hirenzaki *et al.* [5] which the halo potential due to two weakly bound neutrons is assumed to have only an imaginary part within the Born approximation.

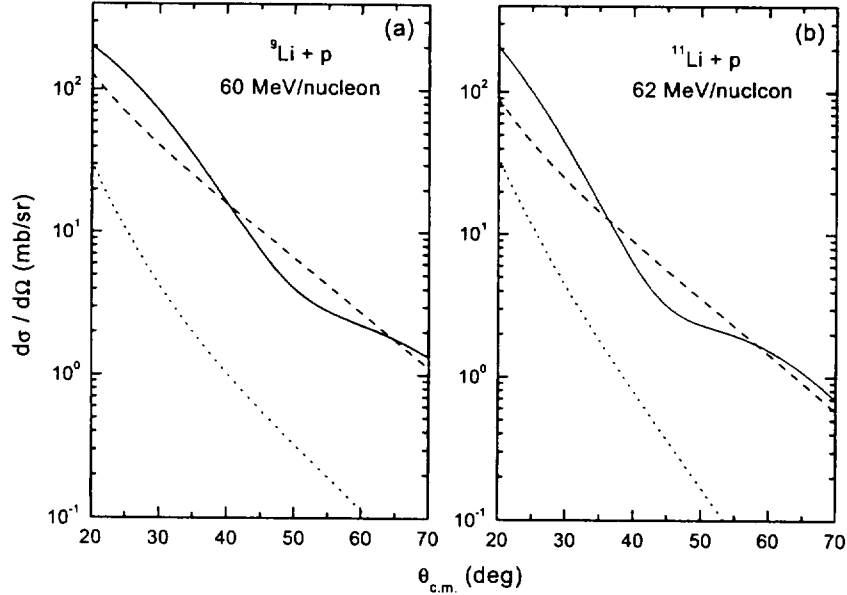


FIG. 2: Differential cross sections (solid curves), near-side contributions (dotted curves), and far-side contributions (dashed curves) following the Fuller's formalism [22] from the the Coulomb-modified eikonal model based on hyperbolic trajectory. The Fig. 2(a) are the calculated results obtained from the common Coulomb-modified eikonal model, while the Fig. 2(b) is the calculated one using the Coulomb-modified eikonal model including the halo effect.

IV. CONCLUDING REMARKS

In this paper, we have presented the Coulomb-modified eikonal model based on hyperbolic trajectory taking into account the halo effect. It has been applied to the elastic scattering of $^{11}\text{Li}+p$ system at $E_{\text{lab}}/A = 62$ MeV/nucleon. By treating ^{11}Li as halo structure, the nuclear optical potential is assumed as a sum of core and two halo neutrons, indicating that phase shift can be given as a

sum of core nucleus and two halo neutrons contributions. The elastic cross sections for $^{11}\text{Li}+p$ system at $E_{\text{lab}}/A=62$ MeV/nucleon are calculated with the core potential fitted to the $^9\text{Li} + p$ scattering data at $E_{\text{lab}}/A=60$ MeV/nucleon plus the halo potential. The differential scattering cross sections obtained from the calculation including the halo effect improve the agreements with the experimental data for $^{11}\text{Li}+p$ system at $E_{\text{lab}}/A = 62$ MeV/nucleon, compared to the calcu-

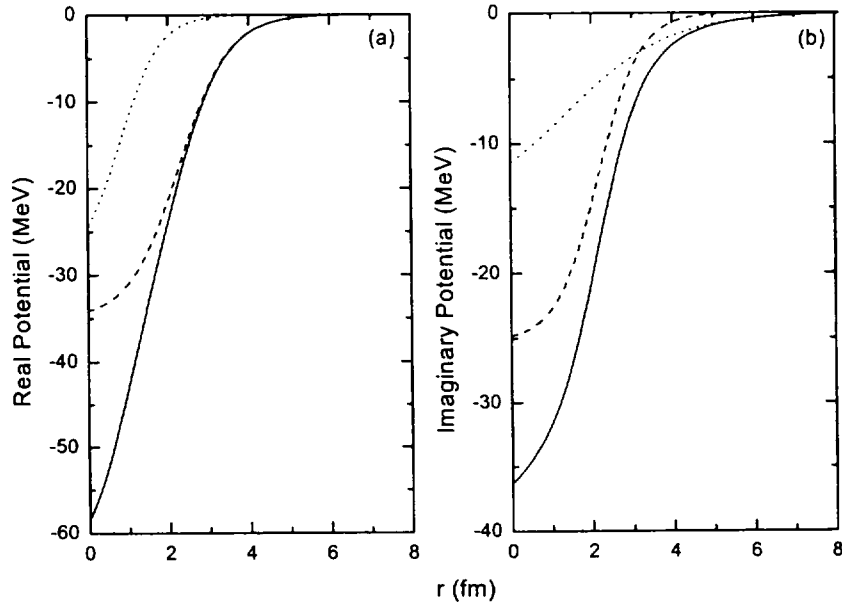


FIG. 3: (a) Real and (b) imaginary parts of optical potential obtained from the Coulomb-modified eikonal model based on hyperbolic trajectory. The solid, dashed and dotted curves correspond to the total, core and halo optical potentials, respectively, for the $^{11}\text{Li}+p$ system at $E_{\text{lab}}/A=62$ MeV/nucleon.

lated result without halo one. A Fuller's decomposition of the elastic cross section into near- and far-side components for the $^9\text{Li}+p$ and $^{11}\text{Li}+p$ systems at $E_{\text{lab}}/A=60$ and 62 MeV/nucleon, respectively, showed that the elastic cross sections are both dominated by the far-side amplitude, indicating very weak oscillation structures of the angular distributions. The real part of halo potential is negligibly small meaning that the elastic cross sections are not sensitive to the real halo potential. However, the imaginary part of halo

potential is significant in the outer regions of imaginary potential.

In conclusion, good agreement of $^{11}\text{Li}+p$ system between the observed data and theoretical result means that the halo neutrons have a large probability to be found outside the interaction range. The two halo neutrons are very weakly bound to the core and are thrown away by collisions. The break-up effect is important to understand the elastic cross section of $^{11}\text{Li}+p$ system at $E_{\text{lab}}/A=62$ MeV/nucleon.

-
- [1] I. Tanihata, *et al.*, Phys. Lett. B **160**, 380 (1985).
 [2] I. Tanihata, *et al.*, Phys. Lett. B **287**, 307 (1992).
 [3] C. B. Moon, *et al.*, Phys. Lett. B **297**, 39 (1992).
 [4] K. Yabana, Y. Ogawa and Y. Suzuki, Phys. Rev. C **45**, 2909 (1992).
 [5] S. Hirenzaki, H. Toki and I. Tanihata, Nucl. Phys. A **552**, 57 (1993).
 [6] M. Kohno, Phys. Rev. C **48**, 3122 (1993).
 [7] A. K. Chaudhuri, Phys. Rev. C **49**, 1603 (1994).
 [8] R. Crespo, J.A.Tostevin and I.J.Thompson Phys. Rev. C **54**, 1867 (1996).
 [9] O.R.Kakuee, *et al.*, Nucl. Phys. A **728**, 339

- (2003).
- [10] B. Abu-Ibrahim and Y. Suzuki, Phys. Rev. C **70**, 011603 (2004).
 - [11] Y. J. Kim and M. H. Cha, J. Korean Phys. Soc. **28**, 712 (1995).
 - [12] T. W. Donnelly, J. Dubach and J. D. Walecka, Nucl. Phys. Nucl. Phys. **A232**, 355 (1974).
 - [13] D. Waxman, C. Wilkin, J. -F. Fermond and R. J. Lombard, Phys. Rev. C **24**, 578 (1981).
 - [14] C. K. Chan, P. Suebka and P. Lu P, Phys. Rev. C **24**, 2035 (1981).
 - [15] D. M. Brink, *Semi-Classical Methods for Nucleus-Nucleus Scattering* (Cambridge Univ. Press, Cambridge, 1985) p.37.
 - [16] C. E. Aguiar, F. Zardi, and A. Vitturi, Phys. Rev. C **56**, 1511 (1997).
 - [17] M. H. Cha and Y. J. Kim, Phys. Rev. C **51**, 212 (1995).
 - [18] S. K. Charagi, Phys. Rev. C **48** 452 (1993).
 - [19] S. K. Gupta and P. Shukla, Phys. Rev. C **52**, 3212 (1995).
 - [20] Y. J. Kim and M. H. Cha, Int. J. Mod. Phys. E **13**, 439 (2004).
 - [21] Y. J. Kim and M. H. Cha, Int. J. Mod. Phys. E **10**, 91 (2001).
 - [22] R. C. Fuller, Phys. Rev. C **12**, 1561 (1975).